ELSEVIER

Carbohydrate Research 316 (1999) 138–154

CARBOHYDRATE RESEARCH

# Extracellular polysaccharide of *Erwinia chrysanthemi* CU643

Byung Yun Yang, James S.S. Gray, Rex Montgomery *

*Department of Biochemistry, College of Medicine, University of Iowa, Iowa City, IA 52242, USA*

Received 9 July 1998; accepted 9 February 1999

**Abstract**

*Erwinia chrysanthemi* are gram-negative bacterial phytopathogens causing soft rots in a number of plants. The structure of the extracellular polysaccharide (EPS) produced by *E. chrysanthemi* strain CU643, pathogenic to Philodendron, has been determined using a combination of chemical and physical techniques including methylation analysis, high- and low-pressure gel-filtration and anion-exchange chromatography, high-pH anion-exchange chromatography, partial acid hydrolysis, mass spectrometry, and 1- and 2-D NMR spectroscopy. In contrast to the structures of the EPS reported for other strains of *E. chrysanthemi*, the EPS from strain CU643 is a linear polysaccharide containing L-Rha*p*, D-Gal*p*, and D-GlcA*p* in the ratio 4:1:1. Evidence is presented for the following hexasaccharide repeat unit:

→3)-β-D-Gal*p*-(1→2)-α-L-Rha*p*-(1→4)-β-D-GlcA*p*-(1→2)-α-L-Rha*p*-(1→2)-α-L-Rha*p*-(1→2)-α-L-Rha*p*-(1→ (**1**)



*Keywords:* *Erwinia chrysanthemi*; Philodendron; Extracellular polysaccharide; Structure

## 1. Introduction

*Erwinia chrysanthemi* spp. are Gram-negative bacterial phytopathogens that cause soft rot in a number of plants [1–6]. Many of the *E. chrysanthemi* spp. produce copious amounts of extracellular polysaccharide (EPS), the role of which in host-specificity and virulence is not known. Also, little is known about the structures of the EPS produced by strains of *E. chrysanthemi* other than those determined for the corn pathogen, SR 260 [7,8], and the potato pathogens, Ech6 [9], Ech1 and Ech9 [10]. As part of a systematic study of the structures of the EPS produced by *E. chrysanthemi*, the structure of an EPS from strain CU643, a pathogen of Philodendron, is presented here.

## 2. Experimental

*Production and purification of polysaccharide.*—*E. chrysanthemi* strain CU643, originally isolated from Philodendron, was the gift of Dr E.J. Braun, Department of Plant Pathology, Iowa State University, Ames, Iowa. EPS was produced on a modified Scott's medium solidified with 1.5% agar (Difco Laboratories, Detroit, MI), supplemented with 1.5% glucose, and isolated as described previously [7,9]. The crude EPS was dialyzed against three changes of distilled wa-

* Corresponding author. Fax: +1-319-335-9570.
*E-mail address:* rex-montgomery@uiowa.edu (R. Montgomery)

0008-6215/99/$ - see front matter © 1999 Elsevier Science Ltd. All rights reserved.
PII: S0008-6215(99)00054-3

ter and lyophilized. The yield of the EPS was about 450 mg $L^{-1}$ of medium and contained 59% carbohydrate as determined by phenol–$H_2SO_4$ [11].

Crude CU643 EPS (2 mg $mL^{-1}$ in phosphate-buffered saline, PBS, pH 7.3) was purified by fractional precipitation with acetone followed by low-pressure gel-permeation and anion-exchange chromatographies. Gel filtration was performed on a ToyoPearl HW65F column (1.5 × 100 cm, TosoHaas, Montgomeryville, PA), eluting with 1% NaCl, where the EPS eluted as a broad peak with a molecular weight $>66$ kDa, using a dextran standard. Fractions were pooled appropriately and chromatographed on a ToyoPearl DEAE-650M (TosoHaas, Montgomeryville, PA) anion-exchange column (1.5 × 15 cm) which had been equilibrated in water and eluted with a linear gradient of 0–500 mM KCl. The EPS eluted as a single peak at about 200 mM KCl. The fractions containing EPS were pooled, electrodialyzed, and lyophilized for further analysis.

CU643 EPS was purified by gel-filtration chromatography for some experiments involving the production of oligosaccharides by partial acid hydrolyses.

*Analytical and general methods.*—The methods used for methylation analysis, GLC and GLC-MS, uronic acid reduction, determination of the absolute configuration of the monosaccharides, monosaccharide analysis by high-pH anion-exchange chromatography with pulsed ampeormatic detection (HPAEC–PAD) and by GLC have been described [7,9,12].

*Partial hydrolysis of EPS by fuming HCl.*—Partial acid hydrolysis with fuming HCl was performed as described previously [12,13] with some modification. Briefly, CU643 EPS (26 mg) was dissolved in 4.6 mL of fuming HCl (37.5%, sp. gr. ≈ 1.19, Fisher Scientific, Pittsburgh, PA) with vigorous stirring and intermittent cooling on ice, warmed to 40 °C and held at this temperature for either 14 or 30 min. The solutions were cooled on ice, neutralized with 2.5 M NaOH (pH paper), diluted with water and lyophilized.

The lyophilized sample was dissolved in water (12 mL), any precipitate removed by centrifugation and then desalted in three batches on a Bio-Gel P-2 column (2.5 × 18 cm, -400 mesh), eluting with water. The oligosaccharide fractions were pooled appropriately, lyophilized, dissolved in water (2 mL) and further purified by chromatography on a Bio-Gel P-4 column (1.5 × 86 cm, 200–400 mesh), eluting with 100 mM $NH_4OAc$.

For the preparation of octasaccharides and dodecasaccharides, the 14 min partial acid hydrolyzate was desalted on Bio-Gel P-2 and

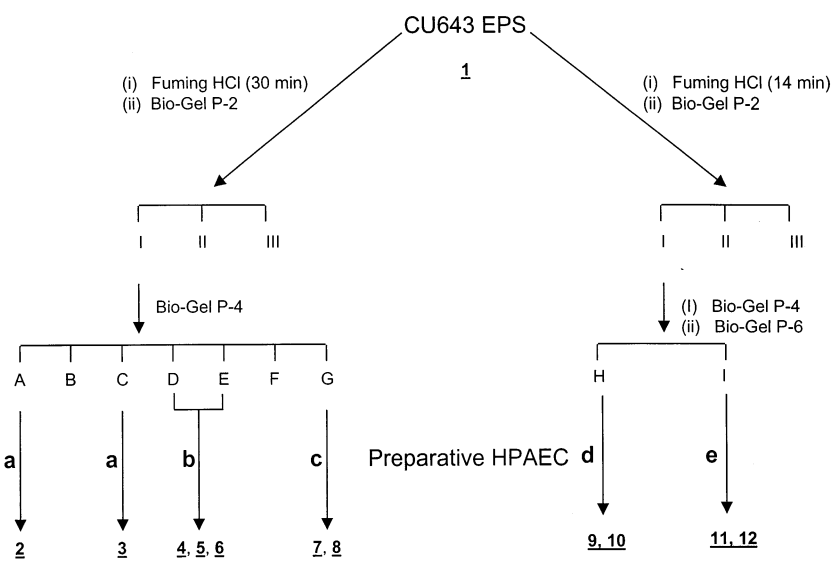


Scheme 1. Oligosaccharides derived by partial acid hydrolysis of *E. chrysanthemi* CU643 EPS with fuming HCl. Preparative HPAEC isocratic elution conditions: (a) 40 mM NaOH–150 mM NaOAc; (b) 40 mM NaOH–140 mM NaOAc; (c) 40 mM NaOH–130 mM NaOAc; (d) 40 mM NaOH–100 mM NaOAc; (e) 50 mM NaOH–140 mM NaOAc.

Table 1
Methylation analyses of *E. chrysanthemi* CU643 EPS and its oligosaccharides[a]

| Methylated sugar[b] | Relative mol ratio | | | | | |
|---|---|---|---|---|---|---|
| | EPS[c] | di[d] | tri | tetra | | penta[e] |
| | **1** | **2** | **3** | **4** | **5** | **6** |
| 1,3,4,5-*O*-$Me_4$Rha | | | 0.5 | 0.6 | 0.6 | 0.2 |
| 2,3,4-*O*-$Me_3$Rha | | | | | | |
| 3,4-*O*-$Me_2$Rha | 4.0 | 1.0 | 1.0 | 2.0 | 1.0 | 3.0 |
| 1,2,4,5,6-*O*-$Me_5$Gal | | | | | | 0.7 |
| 2,3,4,6-*O*-$Me_4$Gal | | | | | 1.2 | |
| 2,4,6-*O*-$Me_3$Gal | 1.0 | | | | | 0.1 |
| 2,3-*O*-$Me_2$Glc(A)[f] | | | | | 0.8 | |
| 2,3,6-*O*-$Me_3$Glc[g] | 1.0 | | | | | |
| 2,3,4-*O*-$Me_3$Glc(A)[h] | | 1.0 | 0.9 | 0.9 | | 0.9 |
| | $m/z$ ($M+Na^+$) | | | | | |
| Observed | | 461.8 | 650.6 | 824.3 | 854.3 | 1028.4 |
| Calculated | | 461.2 | 651.3 | 825.4 | 855.4 | 1029.5 |

[a] *E. chrysanthemi* CU643 EPS was subjected to partial acid hydrolysis with fuming HCl as described in the text and the oligosaccharides were purified by a combination of gel-filtration chromatography on Bio-Gel P-2, Bio-Gel P-4, Bio-Gel P-6 and HPAEC.

[b] 2,3,4-*O*-$Me_3$Rha = 1,5-di-*O*-acetyl-1-deuterio-2,3,4-tri-*O*-methylrhamnitol, etc.

[c] Carboxyl-reduced EPS.

[d] Oligosaccharide methylated.

[e] Pentasaccharide alditol contaminated with a tetrasaccharide alditol ($m/z$ 824.1, 17%), and a hexasaccharide alditol ($m/z$ 1202.5, 16%).

[f] Observed as 1,4,5,6-tetra-*O*-acetyl-1,6,6′-trideuterio-2,3-di-*O*-methylglucitol derived from the reduction of the methyl ester of 2,3-$Me_2$GlcA with superdeuteride.

[g] Observed as 1,4,5-tri-*O*-acetyl-1,6,6′-trideuterio-2,3,6-tri-*O*-methylglucitol.

[h] Observed as 1,5,6-tri-*O*-acetyl-6,6′-dideuterio-2,3,4-tri-*O*-methylglucitol derived from reduction of the methyl ester of 2,3,4-$Me_3$GlcA with superdeuteride.

chromatographed on Bio-Gel P-4 as already noted. The pooled peaks were further fractionated on a Bio-Gel P-6 column (1.5 × 90 cm, 200–400 mesh), eluting with 100 mM $NH_4OAc$. Peaks were pooled appropriately and lyophilized.

*HPAEC purification of acid oligosaccharides.*—Each of the fractions isolated from Bio-Gel chromatography was further fractionated by HPAEC on a CarboPac PA-1 column (4.0 × 250 mm; Dionex Corporation, Sunnyvale, CA). The elution was optimized for isocratic preparative separation for each of the oligosaccharides, eluting with various NaOAc concentrations (see Scheme 1) in the presence of either 40 or 50 mM NaOH. Each fraction that eluted as a single, symmetrical peak, as seen by the PAD, was collected manually and either neutralized immediately with glacial HOAc or reduced with a 30 molar excess of $NaBH_4$. After reduction, the borate was removed by repeated evaporation from 10% HOAc in MeOH and finally from MeOH. A spin column of Bio-Rad AG50W-X8, $H^+$, (0.5–1.0 mL) was used to remove the $Na^+$ from the samples, which were recovered by lyophilization.

The purity of the oligosaccharides and oligosaccharide alditols was analyzed further by HPAEC–PAD on a PA1 CarboPac column (4 × 250 mm) eluting with 40 mM NaOH and either a 50–100 mM NaOAc (oligosaccharide alditols) or a 100–150 mM NaOAc (oligosaccharides) gradient.

The purity of each fraction was checked by matrix assisted laser desorption/ionization-time-of-flight mass spectrometry (MALDI-TOFMS) analysis for the molecular species

present and again after methylation. Linkage analysis of the per-O-methylated oligosaccharide, or its alditol after reduction, established the absence or otherwise of possible glycoisomers.

*Matrix assisted laser desorption/ionization-time-of-flight mass spectrometry and matrix assisted laser desorption/ionization-time-of-flight mass spectrometry-post source decay analyses.*—MALDI-TOFMS was performed on either a Voyager-RP BioSpectrometry Workstation or a Voyager-DE STR BioSpectrometry Workstation (PerSeptive Biosystems, Framingham, MA) operating in the positive-ion mode with an accelerating voltage of 30 or 25 kV, respectively. A total of 2 μL of 2,5-dihydroxybenzoic acid (DHB) (10 mg $mL^{-1}$ in 10% aqueous EtOH) and 1 μL of oligosaccharide in water or per-*O*-methylated oligosaccharide dissolved in EtOH (10–100 pmol) were sequentially loaded onto the target plate, allowed to air-dry and recrystallized from 0.5 μL of absolute EtOH. Maltoheptaose (Boehringer Mannheim, NY) or its per-*O*-methylated derivative were used as external standards.

Post-source decay (PSD) sequencing of the per-*O*-methylated oligosaccharides was performed on a Voyager-DE STR BioSpectrometry Workstation with an accelerating voltage of 25 kV, a grid voltage of 75%, and a guide wire voltage of 0.020–0.000% depending upon the mirror ratio. All analyses were performed with DHB as a matrix.

*Fast-atom bombardment mass spectrometry and liquid secondary ion mass spectrometry of per-O-methylated oligosaccharides.*—Fast atom bombardment mass spectrometry (FABMS) experiments of the per-O-methylated hexasaccharides were performed on a ZAB-HF reversed geometry (BE configuration, where B is a magnetic sector and E is an electrostatic analyzer) mass spectrometer (Micromass, Manchester, UK) equipped with an Ion Tech saddle-field FAB gun and a FAB ion source. Samples were bombarded with 8 keV Xe atoms at an atom gun current of 1.5 mA.

Liquid secondary ion mass spectrometric (LSIMS) analyses of the per-O-methylated octasaccharide alditols were performed on an Autospec mass spectrometer (Micromass) equipped with a LSI ion source. Samples were bombarded with 25 keV $Cs^+$ ions.

The mass spectrometers were calibrated using CsI (Aldrich) or glycerol. Thioglycerol (with and without the addition of 200 mM HCl), glycerol, and 3-nitrobenzyl alcohol were used as matrices. Per-O-methylated oligosaccharide (1–2 μL) in MeOH (0.5–0.7 μg/μL) was added to the matrix on the FAB or LSI probe tip and 3–5 scans were collected for

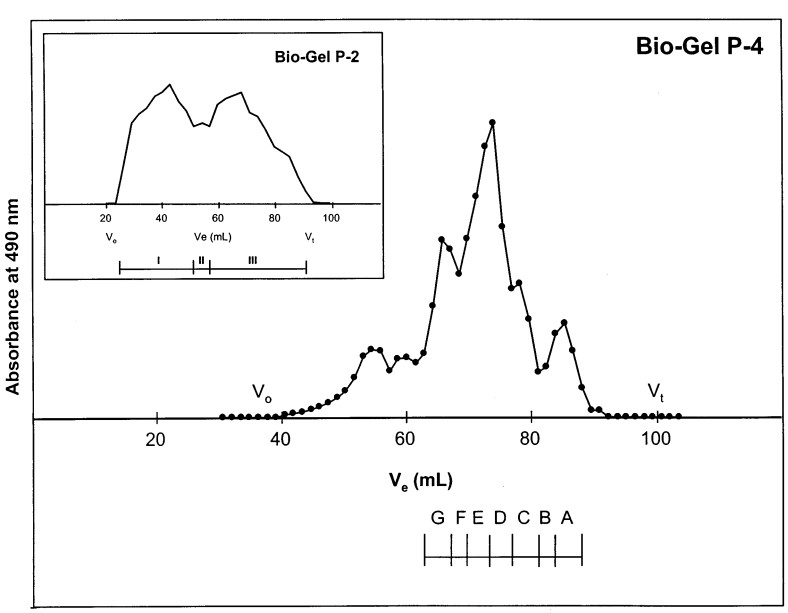


Fig. 1. Chromatography of Bio-Gel P-2 pool I on Bio-Gel P-4 (1.5 × 86 cm). Inset: desalting of the partial acid hydrolyzate (fuming HCl, 30 min, 40 °C) prepared from *E. chrysanthemi* CU643 EPS on a Bio-Gel P-2 column (2.5 × 18 cm).

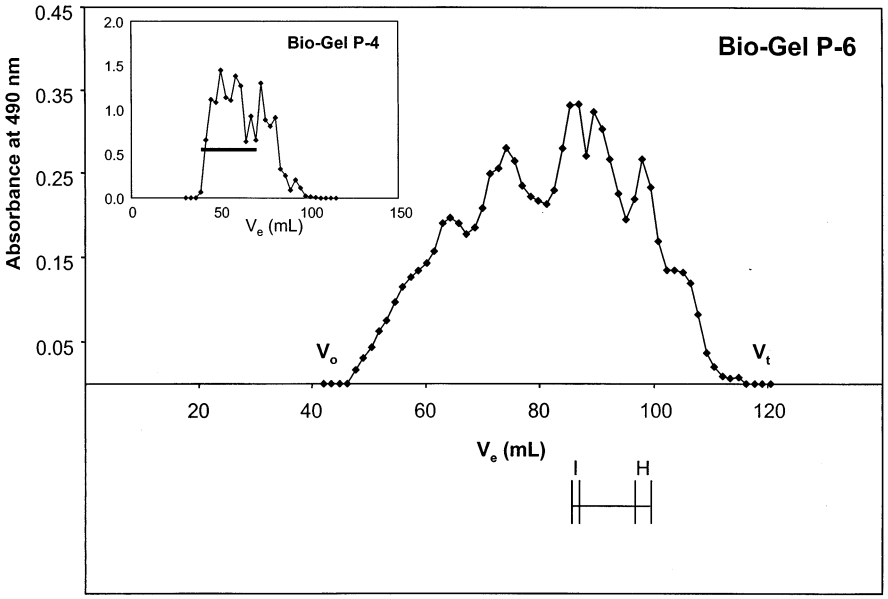


Fig. 2. Chromatography of the Bio-Gel P-4 high-molecular-weight fraction (see inset) on Bio-Gel P-6 (2.5 × 18 cm). Inset: chromatography of the higher-molecular-weight species from a partial acid hydrolyzate of *E. chrysanthemi* CU643 EPS (fuming HCl, 14 min, 40 °C), previously desalted by Bio-Gel P-2, on Bio-Gel P-4 (1.5 × 86 cm). The fractions under the bar were pooled and lyophilized.

each analysis. The data was processed with the Micromass software for the ZAB-HF MS and with OPUS software for the Autospec.

*NMR analyses.*—$^{1}$H NMR 1- and 2-D analyses were acquired on a Bruker AMX-600 NMR spectrometer ($^{1}$H at 600.13 MHz; $^{13}$C at 150.92 MHz). Proton spectra were acquired with a 5-mm proton-only probe using standard Bruker software as described previously [7–9]. NOESY spectra were obtained with a 80 ms mixing time, whereas TOCSY spectra were acquired with a 150 ms mixing time. HMQC and HMBC spectra were acquired with a 5 mm broadband inverse probe with delays of 3.333 and 60 ms, respectively (decoupling optimized for ~150 Hz and ~8 Hz respectively). A 1-D version of the HMQC program without decoupling was used for measurement of the H-1/C-1 ($^{1}J_{\text{H-1-C-1}}$) coupling constants.

All data were processed on a Silicon Graphics O2 with Felix 95.0 (Biosym Technologies, San Diego, CA).

## 3. Results and discussion

*Purification and composition of EPS.*—No low-molecular-weight material or neutral polysaccharides were detected in the crude CU643 EPS and neither protein nor nucleic acids were detected in the purified EPS by UV spectrometry.

Monosaccharide analysis of fractions across the carbohydrate peak from both the gel-filtration and the DEAE-650M columns revealed a similar composition.

Only Rha, Gal, and GlcA were detected in acid hydrolyzates of CU643 EPS by HPAEC–PAD analysis and in methanolyzates by GLC of the trimethylsilyl ($Me_3Si$) derivatives. GLC analysis of the $Me_3Si$ derivatives of the *R*-(−)-butan-2-ol glycosides, as described by Gerwig et al. [14], revealed that Rha was of the L configuration and both Gal and GlcA were of the D configuration. The composition of carboxyl-reduced EPS was found to be L-Rha, D-Gal, and D-Glc in the ratio 4:1:1. The detection of 6,6′-dideuterio-glucitol hexaacetate by GLC-MS provided proof that the Glc is derived from GlcA. Thus, the composition of the native EPS is L-Rha, D-Gal, and D-GlcA in the ratio, 4:1:1.

*Methylation analysis of carboxyl-reduced CU643 EPS.*—Methylation analysis of the $NaBD_4$ carboxyl-reduced EPS disclosed the presence of 2-linked Rha, 3-linked Gal and 4-linked GlcA (detected as 1,4,5-tri-*O*-acetyl-

Table 2
MALDI-TOFMS analyses of the per-O-methylated oligosaccharides purified from partial acid hydrolyzates of *E. chrysanthemi* CU643 EPS by Bio-Gel P-2, Bio-Gel P-4 and Bio-Gel P-6 chromatography (see Scheme 1)

| Bio-Gel fraction | Calculated composition | Relative signal (%) | $m/z$ ($M+Na^+$) | |
|---|---|---|---|---|
| | | | Observed | Calculated |
| A | GlcARha | >80 | 461.8 | 461.2 |
| B | GlcARha | 55 | 460.5 | 461.2 |
| | $GlcA(Rha)_2$ | 45 | 634.4 | 635.3 |
| C | $GlcA(Rha)_2$ | 96 | 634.8 | 635.3 |
| | GlcAGalRha | 4 | 664.7 | 665.3 |
| D | $GlcA(Rha)_2$ | 26 | 634.8 | 635.3 |
| | $GlcA(Rha)_3$ | 53 | 809.0 | 809.4 |
| | $GlcAGal(Rha)_2$ | 21 | 839.2 | 839.4 |
| E | $GlcA(Rha)_3$ | 58 | 808.5 | 809.4 |
| | $GlcAGal(Rha)_2$ | 16 | 838.6 | 839.4 |
| | $GlcAGal(Rha)_3$ | 26 | 1012.5 | 1013.5 |
| F | $GlcA(Rha)_3$ | 8 | 808.1 | 809.4 |
| | $GlcAGal(Rha)_3$ | 76 | 1012.2 | 1013.5 |
| | $GlcAGal(Rha)_4$ | 16 | 1188.2 | 1187.6 |
| G | $GlcAGal(Rha)_4$ | >70 | 1188.1 | 1187.6 |
| H | $GlcA(Gal)_2(Rha)_4$ | 5 | 1392.5 | 1391.7 |
| | $GlcAGal(Rha)_6$ | 20 | 1535.6 | 1535.8 |
| | $GlcA(Gal)_2(Rha)_5$ | 60 | 1565.7 | 1565.8 |
| I | $(GlcA)_2(Gal)_2(Rha)_8$ | >50 | 2304.8 | 2306.1 |

1,6,6′-trideuterio-2,3,6-tri-*O*-methylglucitol) (Table 1). No per-O-methylated alditol acetates arising from a non-reducing terminal residue or from a branch point were detected, indicating that the molecule is linear and of high molecular weight. It is evident from the methylation analysis that all of the residues in the EPS are in the pyranose form.

*Partial acid hydrolysis and purification of oligosaccharides.*—Fuming HCl has been successfully used for the non-specific depolymerization of very viscous solutions of EPS [13] and for the preparation of oligosaccharides [12]. The presence of Rha in the EPS from *E. chrysanthemi* strain CU643 together with the slight elevation in temperature over that reported by Jansson et al. [13] and Kenne et al. [15] gave rise to substantial degradation of the polysaccharide (Figs. 1 and 2). A 30-min digestion at 40 °C converted most of the polymeric material to oligosaccharides smaller than nonasaccharides (Fig. 1, Table 2), whereas a 14 min treatment produced mainly oligosaccharides larger than hexasaccharides (Fig. 2, Table 2).

The presence of only Rha, Gal, and GlcA in the EPS enabled unique monosaccharide compositions to be determined for the oligosaccharides by MALDI-TOFMS analysis of the per-O-methylated derivatives (Table 2). These compositions were confirmed by HPAEC–

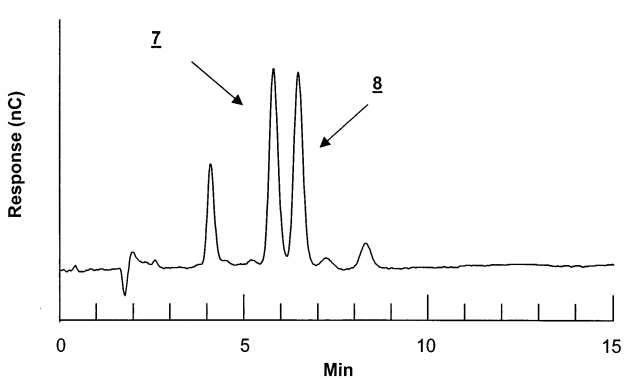


Fig. 3. Purification of hexasaccharides **7** and **8** by HPAEC on a CarboPac PA1 column (4.3 × 250 mm). Isocratic elution with 40 mM NaOH–130 mM NaOAc.

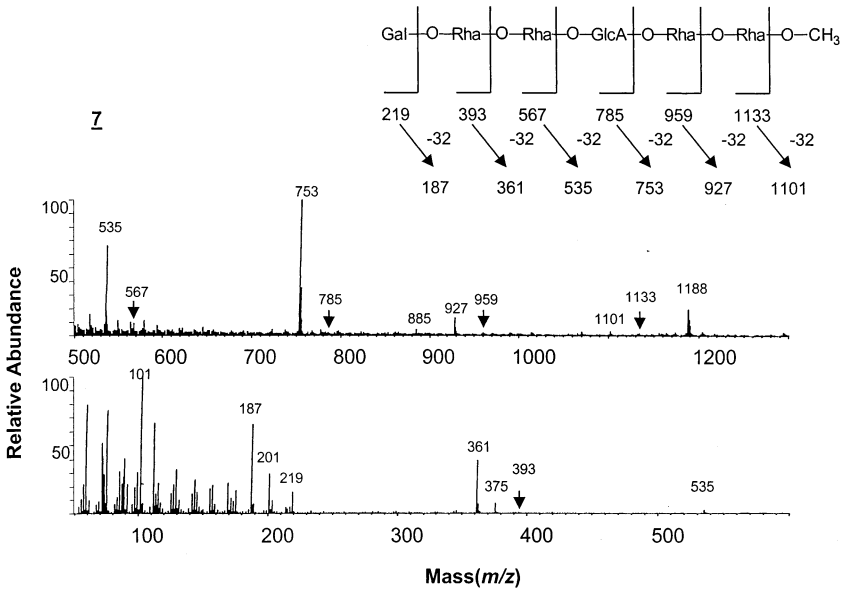


Fig. 4. FABMS analysis of per-O-methylated hexasaccharide **7** on a ZAB-HF mass spectrometer. Samples were bombarded with 8 keV Xe atoms. Two separate analyses were performed, one optimized for the region 50–600 Da (top panel) and the other for the region 500–2500 Da (bottom panel).

PAD analyses of 2 M $CF_3CO_2H$ hydrolyzates of the oligosaccharides. It is evident from Table 2 that all of the Bio-Gel P-4 fractions were mixtures requiring further purification; this was accomplished by preparative HPAEC. The concentration of NaOH during preparative HPAEC was kept low ($\leq 50$ mM) to minimize any alkaline degradation and the NaOAc concentration was varied to obtain the desired separations. Any alkaline degradation was further minimized either by immediately neutralizing the samples or by reduction with solid $NaBH_4$.

The fractionations were followed by MALDI-TOFMS analysis, which alone could not be used as a criterion for purity as some of the fractions contained oligosaccharides with identical molecular weights but different sequences. Before any extensive examination of the fractions, a methylation linkage analysis was conducted to support the purity.

A series of oligosaccharides was thus purified by preparative HPAEC (Scheme 1). An example of the separation of two hexasaccharides, **7** and **8**, from Bio-Gel P-4 fraction G is presented in Fig. 3. The methylation and MALDI-TOFMS analyses of selected purified oligosaccharides are presented in Table 1.

*Sequencing of the oligosaccharides.*—The sequence of each of the purified oligosaccharide fragments from the EPS of CU643 was established principally from mass spectrometry and methylation linkage analysis.

The most intense signals in the FABMS of the per-O-methylated oligosaccharides arose in most cases from A-type cleavages [16–18] followed by loss of methanol; the pseudomolecular ion was observed as the sodium adduct (M + 23) whereas the fragment ions were not. Attempts at sequencing some of the higher oligosaccharides by LSIMS were unsuccessful because internal cleavages result in only the lower-molecular-weight ions being detected.

Matrix assisted laser desorption/ionization-time-of-flight mass spectrometry–post source decay (MALDI-TOFMS-PSD) analyses demonstrated cleavage on both sides of the glycosidic oxygen to give ions of the B-, C-, Y- and Z-series (nomenclature of Domon and Costello [19]; fragmentation mechanisms involving H-migration as described by Rheinhold et al. [20]) with the B- and Y-ions dominating. Although apparently more complex than the FABMS spectra, the analysis was applicable to all oligosaccharides (including the dodecamer that defied LSIMS analysis) and usually provided unambiguous sequences. The complexity of the MALDI-TOFMS-PSD was prominent around uronosyl

residues and sometimes gave rise to ambiguity when these residues were internal in the sequence. This is illustrated below in the MALDI-TOFMS-PSD analyses of two hexasaccharides, **7** and **8**.

*Di-, tri-, and tetrasaccharides*. The sequences of the aldobiuronic (**2**) acid, and the parent aldotriuronic (**3**) and aldotetrauronic (**4**) acids can be deduced directly from their methylation analyses (Table 1) and are as follows:

β-D-GlcA*p*-(1→2)-α-L-Rha*p* (**2**)

β-D-GlcA*p*-(1→2)-α-L-Rha*p*-(1→2)-α-L-Rha (**3**)

β-D-GlcA*p*-(1→2)-α-L-Rha*p*-(1→2)-α-L-Rha*p*-(1→2)-α-L-Rha (**4**)

The non-quantitative recovery of 2-*O*-acetyl-1,3,4,5-tetra-*O*-methylrhamnitol is due to its volatility under the experimental conditions.

Methylation analysis of tetrasaccharidiitol **5** (*m*/*z* 854.3) revealed that a Gal residue is present at the non-reducing end, and a 2-linked rhamnitol residue is present at the reducing end of the molecule (Table 1). Also present was a 1,4-linked GlcA residue (detected as 1,4,5,6-tetra-*O*-acetyl-1,6,6′-trideuterio-2,3-di-*O*-methylglucitol after reduction with superdeuteride), and a 1,2-linked Rha residue. The sequence of this residue was unambiguously determined by MALDI-TOFMS-PSD analysis ($M + Na^+$, 855.7 Da; Y-ions, 245.7, 463.6, 637.7 Da; B-ions, 241.4, 415.5, 633.9 Da; C-ions, 259.6, 433.5, 651.6 Da; Z-ions, 227.5, 447.5, 619.5 Da) and found to be:

β-D-Gal*p*-(1→2)-α-L-Rha*p*-(1→4)-β-D-GlcA*p*-(1→2)-$Rha_{ol}$ (**5**)

*Pentasaccharides*. MALDI-TOFMS analysis of the oligosaccharide alditol derived from fraction **6** reveals three species, the major being the pentasaccharide alditol (*m*/*z* 1028.4, 67%) contaminated with smaller amounts of the tetrasaccharide alditol (*m*/*z* 824.1, 17%) and hexasaccharide alditol (*m*/*z* 1202.5, 16%). Methylation analysis (Table 1) shows that GlcA is the only non-reducing end residue but that Gal and Rha comprise 78 and 22%, respectively, of reducing ends. Together, the MALDI-TOFMS and methylation data are consistent with **6** containing the following related oligosaccharides:

β-D-GlcA*p*-(1→2)-α-L-Rha*p*-(1→2)-α-L-Rha*p*-(1→2)-$Rha_{ol}$ (**6a**) (minor)

β-D-GlcA*p*-(1→2)-α-L-Rha*p*-(1→2)-α-L-Rha*p*-(1→2)-α-L-Rha*p*-(1→3)-β-D-$Gal_{ol}$ (**6b**) (major)

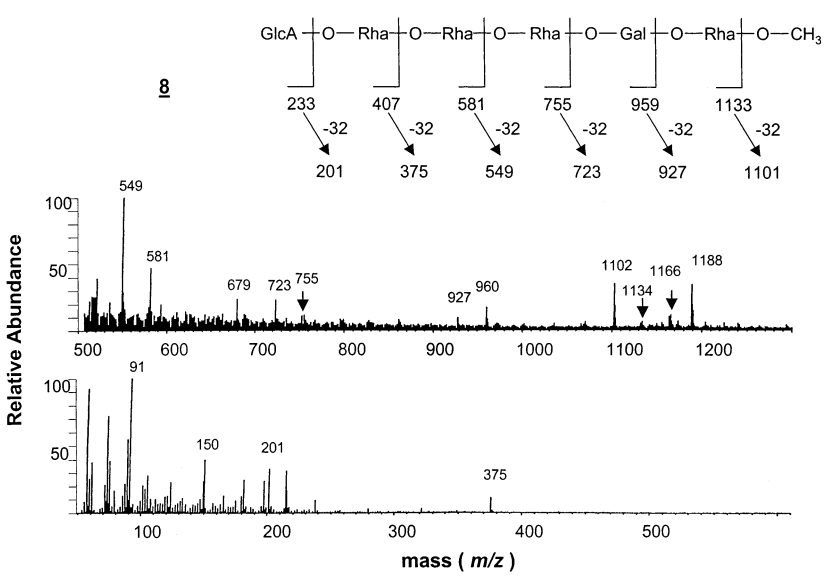


Fig. 5. FABMS analysis of per-*O*-methylated hexasaccharide **8** on a ZAB-HF mass spectrometer. Conditions as for Fig. 4.

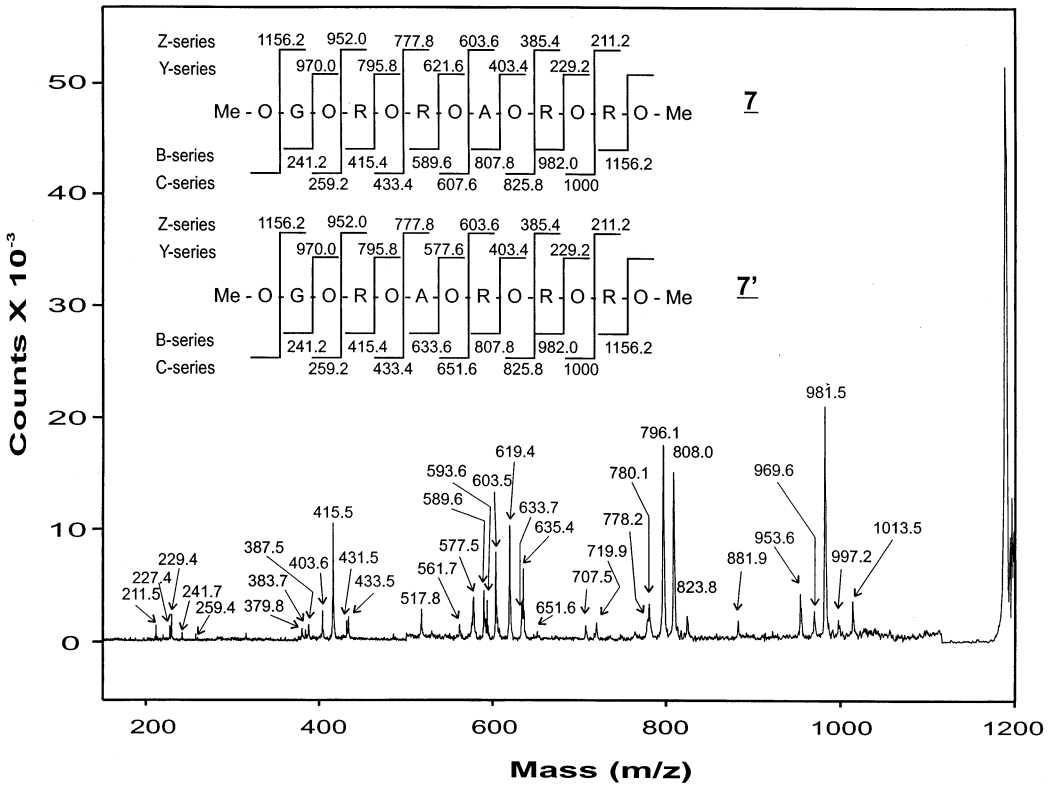


Fig. 6. MALDI-TOFMS-PSD analysis of per-O-methylated hexasaccharide **7**. Abbreviations used are A for GlcA, R for Rha, and G for Gal residues.

*Hexasaccharides*. The monosaccharide composition and masses of the two hexasaccharides, **7** and **8**, were similar. Methylation analyses indicated that **7** was terminated at the non-reducing end by Gal and **8** by GlcA. Both oligosaccharides also contained 1,2-linked Rha residues; additionally, **8** contained a 1,3-linked Gal residue. Methylation analyses of the hexasaccharides revealed that both **7** and **8** contained Rha at the reducing end.

Both **7** and **8** were sequenced by FABMS and MALDI-TOFMS-PSD.

FABMS of the per-O-methyl derivatives of **7** and **8** both gave $[M + Na^+]$ ($m/z$ 1188), $[M + H^+]$ ($m/z$ 1166), and $[M + H^+ - CH_3OH]$ ($m/z$ 1134), the latter being more prominent in the spectrum of **8** (Figs. 4 and 5). The most intense signals were from A-type cleavages followed by the loss of methanol (Figs. 4 and 5). The FAB mass spectra suggest the following sequences for **7** and **8**:

β-D-Gal*p*-(1 → 2)-α-L-Rha*p*-(1 → 4)-
β-D-GlcA*p*-(1 → 2)-α-L-Rha*p*-(1 → 2)-
α-L-Rha*p*-(1 → 2)-α-L-Rha*p* (**7**)

β-D-GlcA*p*-(1 → 2)-α-L-Rha*p*-(1 → 2)-
α-L-Rha*p*-(1 → 2)-α-L-Rha*p*-(1 → 3)-
β-D-Gal*p*-(1 → 2)-α-L-Rha*p* (**8**)

MALDI-TOFMS-PSD analysis of per-O-methylated **7** and **8** are presented in Figs. 6 and 7. In contrast to FABMS, the fragment ions are observed as their sodium adducts $[M + Na^+)]$. The position of the uronic acid plays a significant role in determining the fragmentation pattern.

The MALDI-TOFMS-PSD spectrum of **8**, in which the GlcA is at the non-reducing end, displays a well-defined, dominant series of B- and Y-ions. An unambiguous sequence, **8**, identical to that derived from the FABMS analysis was assigned (Fig. 7). C- and Z-ions of low intensity are also observed in the spectrum. Additional ions, some of which are marked with an asterisk in Fig. 7, arise from further fragmentation of these primary ions.

The MALDI-TOFMS-PSD spectrum of **7** is considerably more complex (Fig. 6). The fragment ions, with good mass accuracy, provide sequence for the leading two sugar residues (Gal → Rha →) and the two tailing residues

($\rightarrow$Rha$\rightarrow$Rha$_{ol}$) (Fig. 6). The complexity, particularly in the region about the uronic acid (Fig. 6), presents some ambiguity in the interpretation of the sequence for **7** for which there is perhaps stronger evidence for the alternative sequence, **7′** (Fig. 6).

*Octasaccharides*. Two octasaccharide alditols, **9** and **10**, were obtained by reduction of the octasaccharides purified by preparative HPAEC from Bio-Gel P-6 fraction H (Scheme 1).

The per-O-methylated oligosaccharide alditol **9** was found to have a mass of 1551.2 Da [M + Na$^+$], in good agreement with the mass of 1551.8 Da calculated for an oligosaccharide alditol containing five Rha residues, one Rha-ol residue, one Gal residue, and one GlcA residue. The presence of Rha-ol at the reducing end was confirmed by methylation analysis, which also revealed that an Rha residue was present at the non-reducing end. Similar analyses determined that octasaccharide alditol **10** contained four Rha residues, one Rha-ol residue, two Gal residues and one GlcA residue. Moreover, methylation revealed that Gal was present at the non-reducing and Rha-ol at the reducing end of **10**.

Per-O-methylated octasaccharide alditols **9** and **10** were sequenced by LSIMS (FABMS) with 3-nitrobenzyl alcohol or thioglycerol as matrices. Both matrices produced strong pseudomolecular ions. Per-O-methylated octasaccharide alditol, **9**, gave pseudomolecular ion signals, *m/z* 1552 [M + Na$^+$], 1530 [M + H$^+$], and 1512 [M + H$^+$ − H$_2$O]; **10** gave *m/z*, 1582 [M + Na$^+$], 1560 [M + H$^+$], and 1542 [M + H$^+$ − H$_2$O]. A strong unassigned signal was observed in the mass spectrum of **10** at *m/z* 1172 with 3-nitrobenzyl alcohol as the matrix; this disappeared when thioglycerol was used as a matrix and therefore arises either from the matrix or is an artifact. Analysis of the fragment ions for **9** and **10** (Fig. 8) was consistent with the following structures:

α-L-Rha*p*-(1 → 2)-α-L-Rha*p*-(1 → 3)-
β-D-Gal*p*-(1 → 2)-α-L-Rha*p*-(1 → 4)-
β-D-GlcA*p*-(1 → 2)-α-L-Rha*p*-(1 → 2)-
α-L-Rha*p*-(1 → 2)-α-L-Rha$_{ol}$ (**9**)

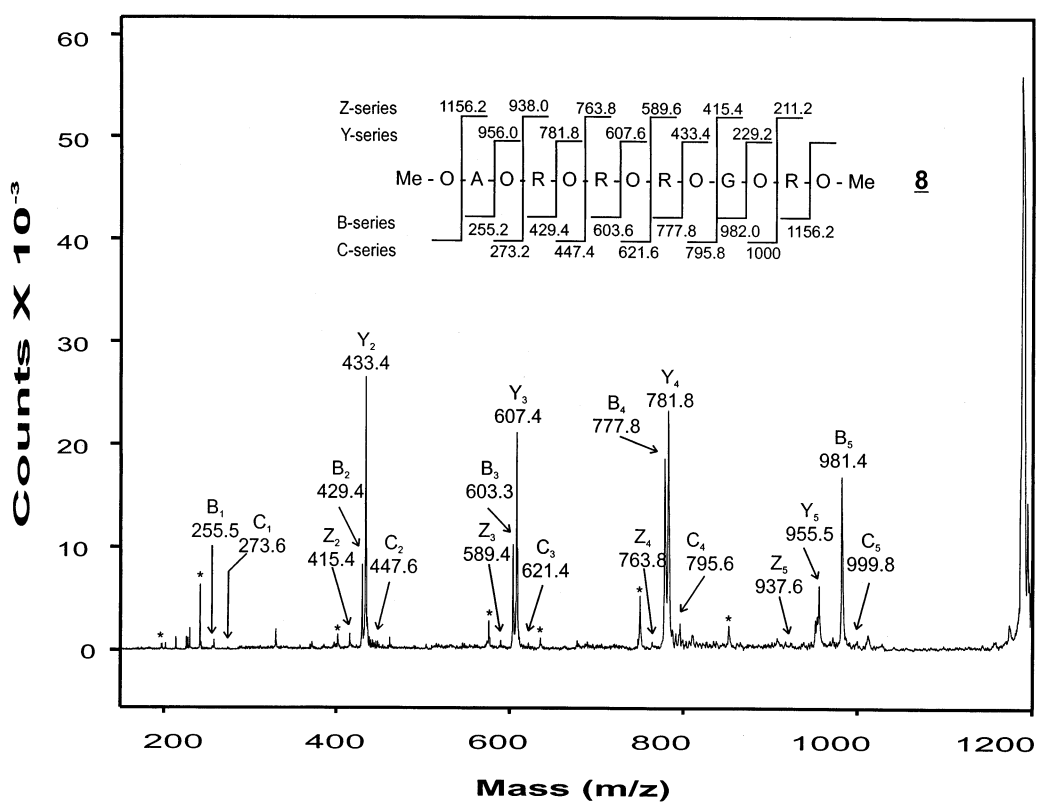


Fig. 7. MALDI-TOFMS-PSD analysis of per-O-methylated hexasaccharide **8**. Abbreviations used are A for GlcA, R for Rha, and G for Gal residues.

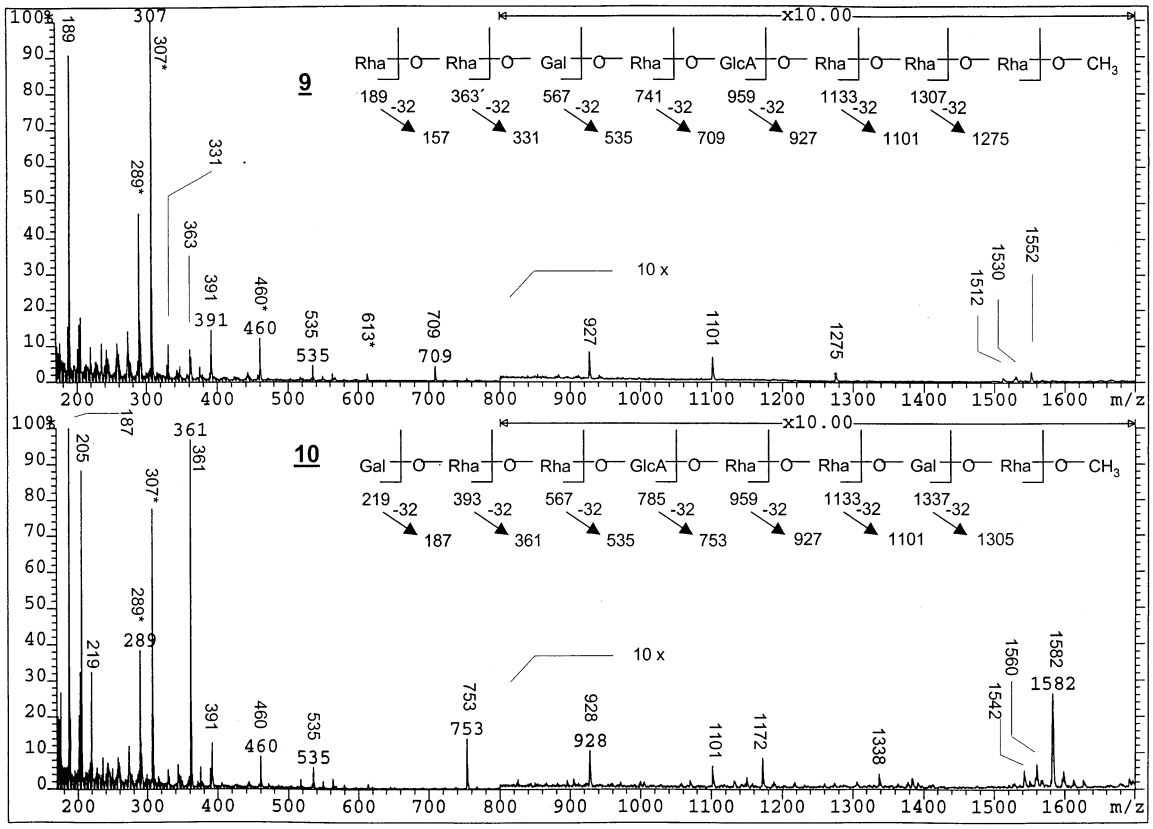


Fig. 8. LSIMS analysis of per-O-methylated octasaccharide alditols **9** and **10** on an Autospec mass spectrometer. Samples were bombarded with 25 keV $Cs^+$.

β-D-Gal*p*-(1→2)-α-L-Rha*p*-(1→2)-α-L-Rha*p*-(1→4)-β-D-GlcA*p*-(1→2)-α-L-Rha*p*-(1→2)-α-L-Rha*p*-(1→3)-β-D-Gal*p*-(1→2)-α-L-$Rha_{ol}$ (**10**)

The sequence of **9** was confirmed by MALDI-TOFMS-PSD analysis, but similar efforts to sequence **10** were unsuccessful, complex spectra being recorded.

*Dodecasaccharides.* Two dodecasaccharide alditols, **11** and **12**, were produced by reduction of the corresponding oligosaccharides purified by HPAEC from Bio-Gel P-6 fraction I (Fig. 2). Both **11** and **12** had similar molecular weights ($M + Na^+$ 2323.3 and 2322.5 Da, respectively) corresponding to the presence of eight Rha residues, two Gal residues, and two GlcA residues (one of which is present as the alditol).

Methylation analysis of **11** revealed that it terminated at the reducing end with 2-linked $Rha_{ol}$ and at the non-reducing end with Gal. The methylation analysis reflects that of CU643 EPS and provides evidence for seven 1,2-linked Rha residues, two 1,4-linked GlcA residues and one 1,3-linked Gal residue in addition to the two residues mentioned above. Methylation analysis of **12** disclosed the presence of 2-linked $Rha_{ol}$ at the reducing end and GlcA at the non-reducing end. Also present were seven 1,2-linked Rha residues, one 1,4-linked GlcA residue, and two 1,3-linked Gal residues.

Attempts at sequencing **11** and **12** by LSIMS were unsuccessful, poor intensity of the pseudomolecular ion being observed. This was attributed to internal cleavage of these molecules by the high energy $Cs^+$ (25 keV) used in the ionization process.

Since the MALDI-TOFMS-PSD analysis of **8** (in which the GlcA was at the non-reducing terminal) generated strong sequencing ions that gave an unambiguous sequence for the hexamer (Fig. 7), dodecasaccharide alditol **12**, which was similarly terminated (Fig. 9), was analyzed in the same way. In contrast to the situation in the LSIMS analysis, strong sequencing ions covering the entire molecule

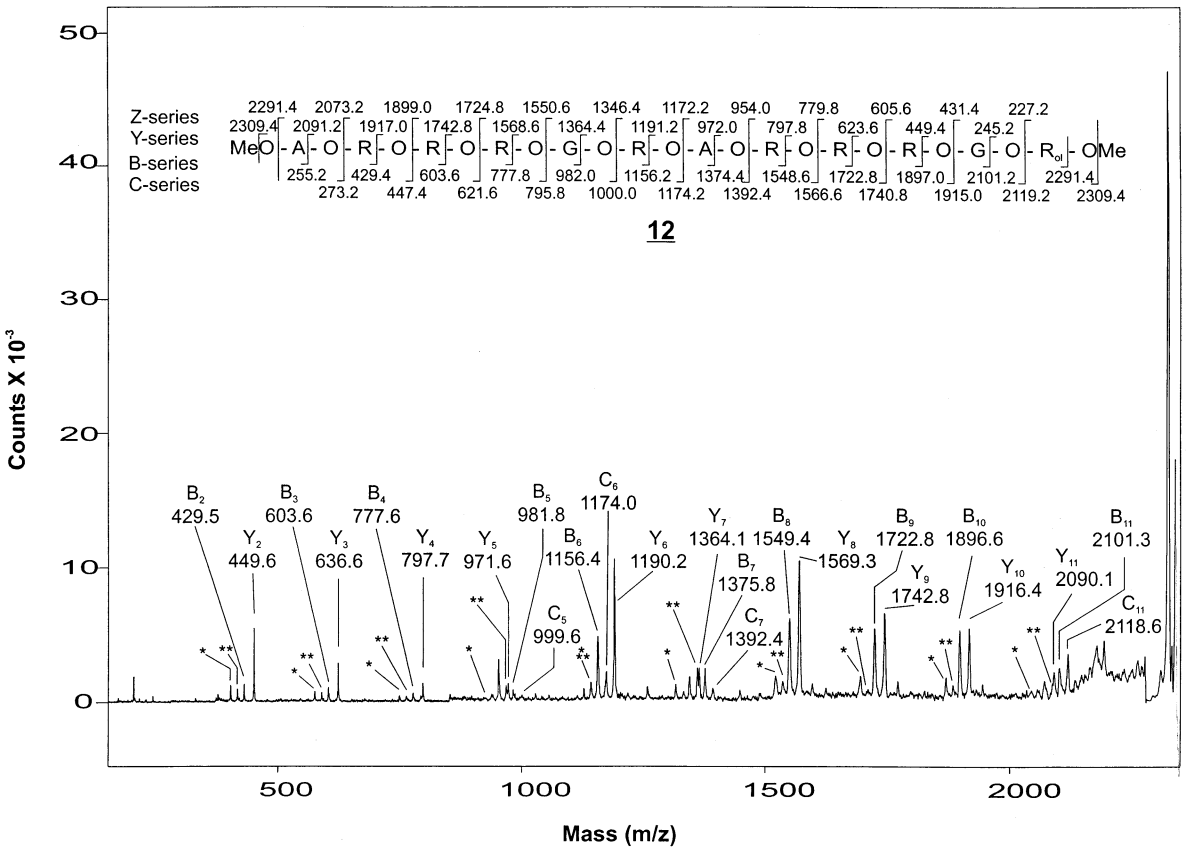


Fig. 9. MALDI-TOFMS-PSD analysis of per-O-methylated hexasaccharide **12**. Abbreviations used are A for GlcA, R for Rha and G for Gal residues. Peaks marked with a single asterisk are derived from further fragmentation of the primary Y-series ions and those marked with a double asterisk are derived from B-series ions.

were observed. A series of intense ions belonging to the Y- and B-series could be assigned with good mass accuracy to give the sequence of **12** (Fig. 9, inset). The presence of the C- and Z-ions of lower intensity was also observed, confirming the sequence elucidated from the B- and Y-ions. Some of the C- and Y-ions are of similar mass, e.g. $C_4$ and $Y_4$ (795.9 and 797.9 Da, respectively), and so are difficult to distinguish, particularly as the Y-ions are in general more intense than the C-ions. Nonetheless, $C_5$, $C_6$, $C_7$, and $C_{11}$ were sufficiently removed from the masses of the Y-ions to be distinguished (999.6 vs. 971.6 Da, 1174.0 vs. 1190.2 Da, 1392.5 vs. 1364.1 Da, 2118.6 vs. 2090.1 Da, respectively). The Z-ions are not observed in the spectrum either because their masses are close to many of the B-series masses or because they are of low intensity. The additional peaks observed in the PSD spectrum could be largely rationalized as arising from further fragmentation of the Y-ions and B-ions. Peaks marked with a single asterisk in Fig. 9 can be rationalized as secondary fragments derived from further fragmentation of the Y-series ions, whereas those labeled with a double asterisk arise from B-series ions.

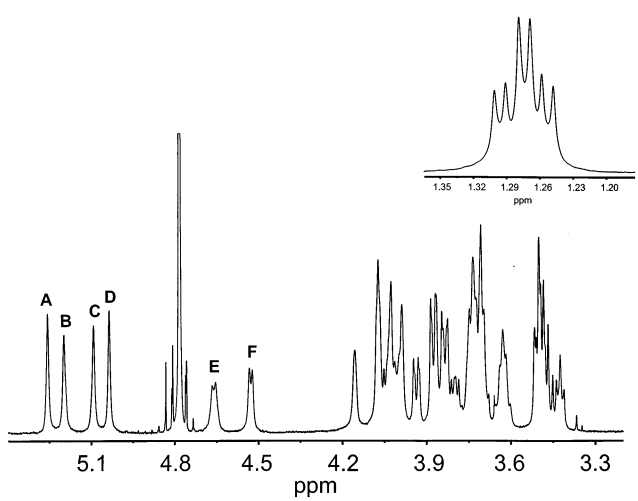


Fig. 10. 1-D $^1$H NMR spectrum of native *E. chrysanthemi* CU643 EPS recorded in $D_2O$ at 600 MHz and 298 K. Inset: 6-deoxy region of the spectrum.

Table 3
Assignment of the $^1H$ and $^{13}C$ resonances for *E. chrysanthemi* CU643 EPS[a]

→1)-β-D$_E$GlcA*p*-(1→2)-α$_A$-L-Rha*p*-(1→2)-α$_C$-L-Rha*p*-(1→2)-α$_B$-L-Rha*p*-(1→3)$_F$β-D-Gal-(1→2)-α$_D$-L-Rha*p*-(1→

| Residue | $\delta_H$ and $\delta_C$ (ppm)[b] | | | | | | |
|---|---|---|---|---|---|---|---|
| | **1** | **2** | **3** | **4** | **5** | **6a** | **6b** |
| A, →2)-α-L-Rha*p*-(1→ | 5.258<br>101.7 | 4.156<br>81.1 | 3.876<br>70.6 | 3.501<br>72.9 | 3.73<br>71.0 | 1.273<br>17.4 | |
| B, →2)-α-L-Rha*p*-(1→ | 5.201<br>101.4 | 4.07<br>78.9 | 3.938<br>70.7 | 3.494<br>72.9 | 3.80<br>70.5 | 1.295<br>17.5 | |
| C, →2)-α-L-Rha*p*-(1→ | 5.093<br>101.6 | 4.08<br>78.9 | 3.876<br>70.6 | 3.468<br>72.8 | 3.70<br>70.1 | 1.273<br>17.4 | |
| D, →2)-α-L-Rha*p*-(1→ | 5.037<br>100.7 | 4.027<br>80.7 | 3.836<br>70.5 | 3.501<br>72.9 | 4.03<br>69.8 | 1.252<br>17.3 | |
| E, →1)-β-D-GlcA*p*-(1→ | 4.661<br>104.9 | 3.425<br>74.3 | 3.618<br>74.6 | 3.63<br>79.7 | 3.99<br>74.8 | | |
| F, →3)-β-D-Gal-(1→ | 4.531<br>105.4 | 3.694<br>71.8 | 3.71<br>79.9 | 3.99<br>69.3 | 3.75<br>76.1 | 3.75<br>62.0 | 3.84<br>62.0 |

[a] COSY, TOCSY and HMQC spectra were acquired and analyzed as described in the text.
[b] Proton chemical shifts derived from 1-D spectrum where possible (3 decimal places, error ±0.002 ppm); in very crowded regions, proton chemical shifts derived directly from COSY cross-peaks (2 decimal places, error ±0.01 ppm). Carbon chemical shifts derived from HMQC spectrum (error ±0.1 ppm).

An attempt to sequence **11** in the same way was unsuccessful and is the subject of further study.

*$^1H$ NMR analysis of CU64 EPS.*—The study of the sequences of the oligosaccharides gave strong evidence for the sequence **1**, but some of the oligosaccharides offered the possibility of the existence of a second hexameric sequence. These ambiguities were resolved by $^1H$ NMR analysis of CU643 EPS.

Inspection of the integrated 600 MHz $^1H$ NMR spectrum of CU643 EPS obtained at 298 K reveals six anomeric protons, which were labeled A–F from high to low $\delta$, i.e., low to high field (Fig. 10). Two of the signals (E and F) at $\delta$ 4.672 (1 H, $J_{1,2}$ 7.9 Hz) and at $\delta$ 4.536 (1 H, $J_{1,2}$ 6.9 Hz) are characteristic of the β-*gluco* or β-*galacto* configuration and must therefore arise from the D-Gal and D-GlcA residues. The four unresolved resonances at $\delta$ 5.217, 5.190, 5.091, and 5.076 (A–D) (1 H each, $J_{12}$ unresolved) therefore arise from the Rha residues. Twelve protons ($\delta \approx 1.29$ ppm) are present in the methyl region and arise from the 6-deoxy groups of 4 Rha residues (Fig. 10 inset).

The $^1H$ spectrum of the EPS was completely assigned by a combination of 2-D NMR experiments (Table 3). Analysis of the COSY spectrum enabled the assignment of signals for H-1 to H-3 of Rha residues A–D; the Rha H-4 resonances were assigned in the COSY spectrum after resolution of ambiguities by reference to the TOCSY spectrum (Fig. 11). The H-5 resonances of Rha residues A, C and D were difficult to observe in the 1-D NMR spectrum but can be assigned from the H-4/5 cross-peaks in the COSY and TOCSY spectra. They can also be assigned in the COSY spectrum using the 6-deoxy methyl resonances as entry-points. Similarly, all of the resonances for GlcA-E and for the signals arising from H-1 to H-4 of Gal-F can be assigned. The signal due to H-5 of Gal-F was assigned from the COSY cross-peak between H-4 and H-5 of this residue. The signals arising from H-6a and H-6a of Gal-F were not readily discerned in the proton NMR spectra but can be assigned as the most upfield $^{13}C$ signal in the HMQC spectrum; these cross-peaks provided the chemical shifts for these two protons.

All of the $^{13}C$ resonances for the CU643 EPS were assigned with reference to a HMQC spectrum (Table 3). The downfield shifts ($\sim$ 8–10 ppm) of the $^{13}C$-signals arising from the C-2 atoms of Rha residues A–D, and of the C-4 and C-3 atoms of GlcA and Gal, respectively, indicate their involvement in glycosidic linkages and are consistent with the methylation data (Table 1).

The anomeric configurations of the Rha residues are difficult to assign simply by inspection of the 1-D spectrum. Nonetheless, these residues are all α-linked for the following reasons:

1. The $^{1}H$ chemical shifts observed for the H-5 signals of these residues viz. $\delta$ 4.03, 3.79, 3.73 and 3.70 ppm, are typical of α-linked Rha residues [21–23].
2. A 1-D version of the HMQC experiment acquired with no decoupling gave 1-bond coupling constants ($^{1}J_{CH}$) for C-1/H-1 of the Rha residues values ranging from 170 to 175 Hz and values for the GlcA and Gal residues of about 160 Hz. These values are characteristic of α- and β-linked residues, respectively [24].

A 2-D NOESY experiment was used to sequence the polysaccharide (Fig. 12, Table 4).

Rha-C is on the reducing side of Rha-A as evidenced by the strong inter-residue NOESY cross-peak between H-1 and H-2 of these residues (Fig. 12). A weaker inter-residue NOE between H-1 of Rha-A and H-3 of Rha-C is further evidence for the sequence, Rha-A → Rha-C. There is a weak NOE connectivity between Rha-A H-1 and GlcA-E H-1 suggesting the sequence, GlcA-E → Rha-A. Both of these observations are consistent with reports that NOE contacts may also occur with protons adjacent to those involved in the glycosidic linkage [7,25]. No intra-residue cross-peak between H-1 and H-5 of Rha-A is observed, confirming that this residue is α-linked.

A strong NOE between Rha-B H-1 and Gal-F H-3 and a weak contact between Rha-B H-1 and Gal-F H-4 are observed, providing evidence for the sequence Rha-B → Gal-F.

The NOEs between Rha-C H-1 and Rha-C H-2 and Rha-B H-2 are nearly superimposed due to the close proximity of the signals for these latter two protons (Fig. 12, Table 4) and

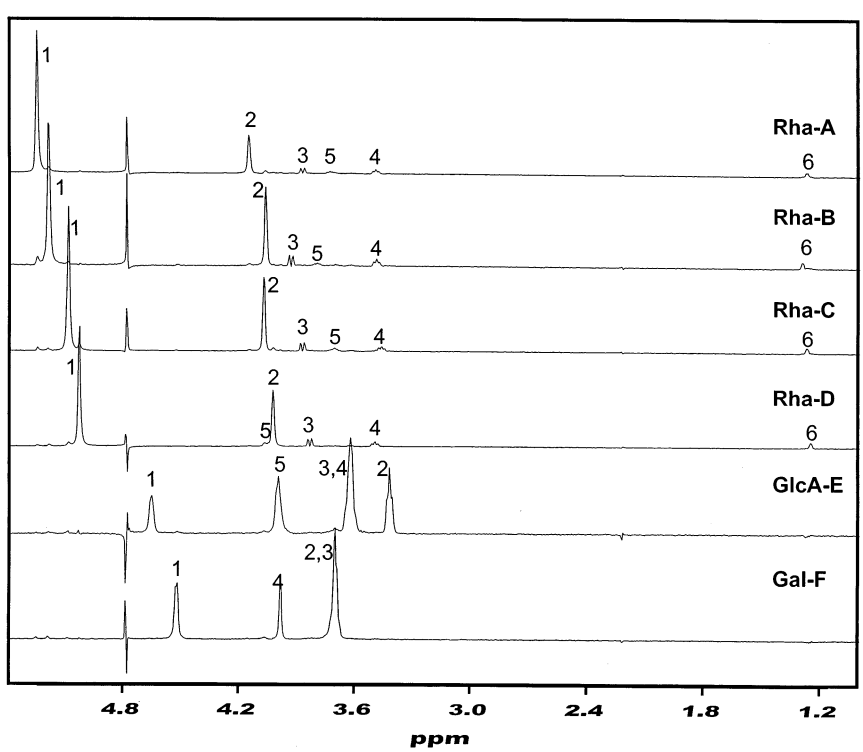


Fig. 11. Sub-spectra through the anomeric protons, A–E, extracted from a 2-D TOCSY $^{1}H$ NMR analysis of CU643 EPS.

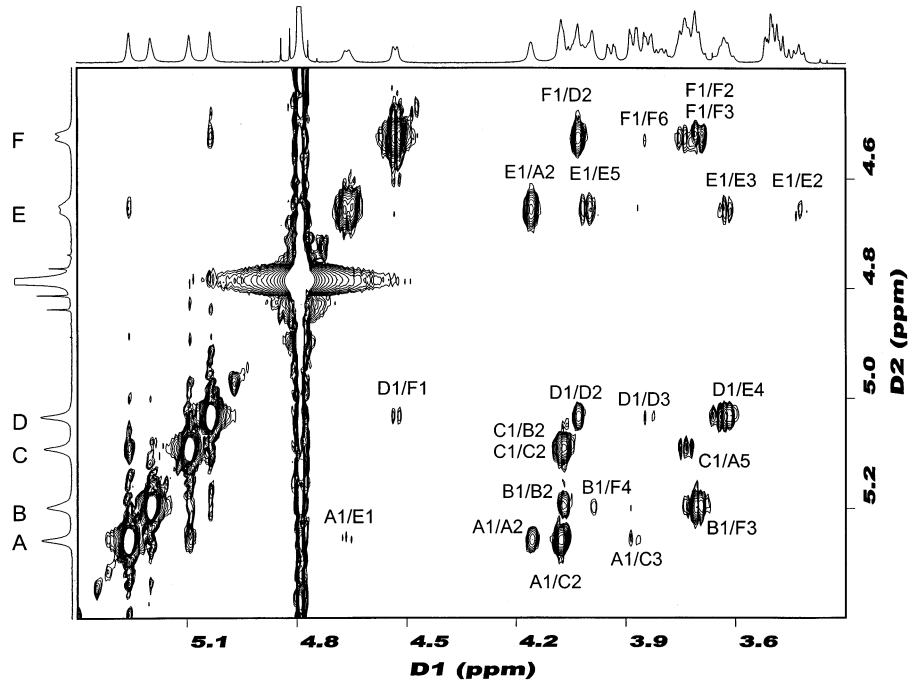


Fig. 12. 2-D NOESY spectrum of CU643 EPS.

provide evidence for the sequence Rha-C→Rha-B. A weak inter-residue NOE between Rha-C H-1 and Rha-A H-5 is also observed and may be due to the adoption of a $^{5}Rha_2$ chair conformation for this residue as described by Widmalm et al. [26].

In addition to a NOE contact between H-1 and H-2 of Rha-D, a strong NOE is observed between H-1 of Rha-D and H-4 of GlcA (Fig. 12), furnishing evidence for the sequence Rha-D→GlcA-E. A weak NOE between H-1 of Rha-D and what is possibly H-6a of Gal-F is also observed.

The H-1 of GlcA-E has a strong NOE with H-2 of Rha-A; it also has intra-residue NOEs with H-2, H-3 and H-5 of GlcA, all of which are predicted to occur for β-linked GlcA. Thus, these data provide evidence for the sequence GlcA-E→Rha-A and establish the β-linkage of the GlcA residue.

A strong inter-residue NOESY cross-peak between H-1 of Gal-F and H-2 of Rha-D is observed, providing evidence for the sequence Gal-F→Rha-D. In addition, intra-residue NOEs between Gal H-1 and Gal H-6a (very weak), and Gal H-2 and Gal H-3 are also seen. The NOE between Gal H-1 and Gal H-3 confirms the β-configuration of the Gal residue.

A 2-D HMBC analysis of the CU643 EPS was of limited value and provided little additional information. The similarity of the $^{13}C$ chemical shifts of the atoms involved in the glycosidic linkages, viz. C-2 and C-3 of the Rha and Gal residues and C-4 of the GlcA residue (Table 3) made it difficult to assign the observed 3-bond interactions with certainty. Moreover, not all of the predicted 2- and 3-bond C–H and H–C couplings were observed in the HMBC spectrum possibly due to their short $T_2$ times, a characteristic of large macromolecules.

All of these NMR data provide strong evidence for an EPS with hexasaccharide **8** as the repeat subunit.

No pyruvate or acetate was detected in the CU643 EPS by $^{1}H$ NMR spectroscopy.

*The sequence of CU643 EPS.*—The linearity of the polysaccharide from CU643 and the high proportion of contiguous Rha residues in the structure (and hence similarities in the oligosaccharides generated by partial acid hydrolysis) presented a challenge in both the generation and purification of oligosaccharides with overlapping sequences. This was partly overcome by the extensive use of preparative HPAEC; nonetheless, difficulty was still experienced in purifying certain isoforms from each other.

The resolution of the sequence of sugar residues in CU643 EPS resulted from the $^1$H NMR analyses. The existence of six anomeric protons was certainly suggestive of a hexameric repeating unit. The existence of an alternate, interposed sequence could not be ruled out by the presence of several oligomers for which a MALDI-TOFMS-PSD study could be interpreted in two ways. However, extensive NMR examination of the EPS gave no evidence of any significant presence of the repeating unit represented by **7**; if such is present, it must be in amounts below that detectable in the NMR study. No evidence for a second polysaccharide has yet been obtained despite careful fractionation of the polysaccharide.

The study of CU643 EPS, with 1,3-linked α-D-galactopyranosyl and 1,4-linked β-D-glucosyluronic residues in a high proportion of 1,2-linked α-L-rhamnosyl residues illustrated several important points:

- The FABMS of large oligosaccharides is not always useful (particularly with the use of high-energy ion beams as in LSIMS) for determining the sequence of large oligosaccharides because of internal cleavages.
- Ions representing cleavage on both sides of the glycosidic bond are produced during MALDI-TOFMS-PSD of methylated oligosaccharides, with the B- and Y-series ions generally more intense than the C- and Z-series ions. In many instances, this allows a sequence to be rapidly proposed, even for fairly large oligosaccharides. Internal cleavages of the oligosaccharides become more prominent with increase in size and provide additional evidence for the interpreted sequence.
- With some oligosaccharides, there could be ambiguities in the interpretation of sugar sequence until the mechanism of MALDI-TOFMS-PSD fragmentation around internal glycosyluronic residues is better understood.
- The isolation of overlapping oligosaccharides is a valuable contribution to the structural study of parent polysaccharides, but the separation of closely related species of the same molecular size needs careful investigation.

Table 4
NOE data for the EPS from *E. chrysanthemi* strain CU643[a]

→1)-β-D-GlcA$p_E$-(1→2)-α-L-Rha$p_A$-(1→2)-α-L-Rha$p_C$-(1→2)-α-L-Rha$p_B$-(1→3)-β-D-Gal$_F$-(1→2)-α-L-Rha$p_D$-(1→

| Residue | Anomeric atom $\delta_H$ | Connectivity to $\delta_H$ | Residue: atom |
|---|---|---|---|
| A, →2)-α-L-Rha*p*-(1→ | 5.258 | 4.157 | A: A-2 |
| | | 4.08 | A: C-2 |
| B, →2)-α-L-Rha*p*-(1→ | 5.201 | 3.707 | B: F-3 |
| | | 3.691 | B: F-2 |
| C, →2)-α-L-Rha*p*-(1→ | 5.093 | 4.073 | C: B-2, C-2 |
| | | 3.734 | C: A-5 |
| D, →2)-α-L-Rha*p*-(1→ | 5.037 | 3.626 | D: E-4 |
| | | 4.027 | D: D-2 |
| E, →1)-β-D-GlcA*p*-(1→ | 4.661 | 4.156 | E: A-2 |
| | | 4.005 | E: E-5 |
| | | 3.618 | E: E-3 |
| | | 3.425 | E: E-2 |
| F, →3)-β-D-Gal-(1→ | 4.531 | 4.027 | F: D-2 |
| | | 3.737 | F: F-5 |
| | | 3.709 | F: F-3 |
| | | 3.690 | F: F-2 |

[a] The conditions used to acquire the spectra are described in the text.

The EPS from strain CU643 is the first *E. chrysanthemi* polysaccharide with a linear sequence. It contains a high proportion of L-Rha in common with the polysaccharides isolated from other strains of *E. chrysanthemi*, SR260, Ech1, Ech9, SR31, and EPS378 [7–10,12] but differs from them in that the GlcA is of the β configuration.

## Acknowledgements

The authors thank the Biotechnology Byproducts Consortium (USDA Grant No. 94-34188-0039) and the Carbohydrate Structure Facility for the use of its equipment. They also thank L. Teesch and D. Lamb for the FABMS analyses and John Snyder for recording the $^1$H NMR spectra and for many discussions.

## References

[1] F. Barras, F. van Gijsegem, A.K. Chatterjee, *Annu. Rev. Phytopathol.*, 32 (1994) 201–234.

[2] A.K. Chatterjee, M.P. Starr, *Annu. Rev. Microbiol.*, 34 (1980) 645–676.
[3] R.S. Dickey, *Phytopathology*, 69 (1979) 324–329.
[4] R.S. Dickey, *Phytopathology*, 71 (1981) 23–29.
[5] R.S. Dickey, C.H. Zumoff, J.K. Uyemoto, *Phytopathology*, 74 (1984) 1388–1394.
[6] R.S. Dickey, L.E. Claflin, C.H. Zumoff, *Phytopathology*, 77 (1987) 426–430.
[7] J.S.S. Gray, J.M. Brand, T.A.W. Koerner, R. Montgomery, *Carbohydr. Res.*, 245 (1993) 271–287.
[8] J.S.S. Gray, T.A. Koerner, R. Montgomery, *Carbohydr. Res.*, 266 (1995) 153–159.
[9] B.Y. Yang, J.S.S. Gray, R. Montgomery, *Int. J. Biol. Macromol.*, 16 (1994) 306–312.
[10] B.Y. Yang, J.S.S. Gray, R. Montgomery, *Int. J. Biol. Macromol.*, 19 (1996) 223–226.
[11] M. Dubois, K.A. Gilles, J.K. Hamilton, P.A. Roberts, F. Smith, *Anal. Chem.*, 28 (1956) 350–356.
[12] B.Y. Yang, J.S.S. Gray, R. Montgomery, *Carbohydr. Res.*, 296 (1996) 183–201.
[13] P.-E. Jansson, G. Widmalm, *Carbohydr. Res.*, 231 (1992) 325–328.
[14] G.J. Gerwig, J.P. Kamerling, J.F.G. Vliegenthart, *Carbohydr. Res.*, 62 (1978) 349–357.
[15] L. Kenne, B. Lindberg, K. Petersson, P. Unger, *Carbohydr. Res.*, 84 (1980) 184–186.
[16] A. Dell, *Adv. Carbohydr. Chem. Biochem.*, 45 (1987) 19–72.
[17] A. Dell, J.E. Thomas-Oates, in C.J. Biermann, G.D. McGinnis (Eds.), *Analysis of Carbohydrates by GLC and MS*, CRC Press, Boca Raton, FL, 1989, pp. 217–235.
[18] A. Dell, A.J. Reason, K.-H. Khoo, M. Panico, R.A. McDowell, H.R. Morris, *Methods Enzymol.*, 230 (1994) 108–132.
[19] B. Domon, C.E. Costello, *Glycoconjugate J.*, 5 (1988) 397–409.
[20] V.N. Reinhold, B.B. Reinhold, S. Chan, *Methods Enzymol.*, 271 (1996) 377–402.
[21] P.-E. Jansson, L. Kenne, K. Persson, G. Widmalm, *J. Chem. Soc. Perkin Trans. 1*, (1990) 591–598.
[22] P.-E. Jansson, L. Kenne, H. Ottosson, *J. Chem. Soc. Perkin Trans. 1*, (1990) 2011–2018.
[23] P.-E. Jansson, J. Lindberg, K.M.S. Wimalasiri, M.A. Dankert, *Carbohydr. Res.*, 245 (1993) 303–310.
[24] I. Tvaroska, F.R. Taravel, *Adv. Carbohydr. Chem. Biochem.*, 51 (1995) 15–61.
[25] V.K. Dua, B.N.N. Rao, S.-S. Wu, V.E. Dube, C.A. Bush, *J. Biol. Chem.*, 261 (1986) 1599–1608.
[26] G. Widmalm, R.A. Byrd, W. Egan, *Carbohydr. Res.*, 229 (1992) 195–211.